# Chapter 3

# Transportation of micro-polar fluid by dilating peristaltic waves: Application to flows in normal oesophagus

## 3.1 Introduction

Combination of periodically alternating contractions and relaxations of muscles responsible for most of the physiological flows is peristalsis. This combination

The contents of this chapter have been published in **Journal of King Saud University-Science**, **32** (7), (2020)2939-2949.

forms a transverse and progressive wave. This mechanism has several engineering applications. Several innovators, across various fields, are developing peristaltic machines that can move in cylinder tubes to locate ruptures at the joints of gas and water pipelines and those caused by cracks. Many such machines are being designed to serve industries for sanitary fluid transport, blood pumps in heart/lung machines, transport of corrosive fluids without contacting machinery components. Studies are also focused on realization of machines that can pass through the intestines and blood vessels. Peristalsis, observed in earthworms and nematodes, induces shape variation and a shift in the center of gravity. This causes extensional waves to propagate and thus progress without injury to the vulnerable inner walls of blood vessels. This moving mechanism together with catheters can reach a diseased site by itself (Nakazato *et al.*, 2010).

Eringen (1966) formulated the effects of individual particles such as micro-rotation in flow, which are concentrated suspension of non-deformable neutrally buoyant rigid particles in a viscous medium. Micro polar fluids contain micro constituents which can undergo rotation. Rotation of micro constituents can affect the hydrodynamics of flow and make the fluid distinctly non-Newtonian. Physically, micro polar fluids represent fluids consisting of rigid, spherical or randomly oriented particles with ignored deformation suspended in a viscous medium (Grzegorz Lukaszewicz, 1999). Liquid crystals, blood, some edible solutions resemble micro-polar property. Engineering applications using polymer solutions, colloidal solutions, drilling fluids in oil industries etc. may be better understood by this investigation (Pandey and Tripathi, 2011a).

Devi and Devanathan (1975) studied peristaltic transport of micro-polar fluids in a cylindrical tube with a sinusoidal wave of small amplitude. Philip and Chandra (1995) explored peristaltic transport of a simple micro-polar fluid which

accounts for micro-rotation and micro-stretching of the particles contained in a small volume element using long wave length approximations. Srinivasacharya *et al.* (2003) examined different micro-polar properties on pressure across one wavelength and also on trapping; Hayat *et al.* (2007) investigated the effects of different wave forms; Muthu *et al.* (2005, 2008a, b) studied wall properties in channels and tubes respectively whereas Hayat and Ali (2008) prepared effects of an endoscope. The same authors (Ali and Hayat, 2008) studied the effects of asymmetricity of wave propagation of channel while Mekheimer and Elmaboud (2008) studied the flow in an annulus. Asghar *et al.* (2018) used micro-polar fluid to characterize the rheology of a thin layer of slime and its dominant micro-rotation effects. Recently some interesting papers dealing with the flow of micro-organisms such as bacteria cilia driven flows under different condition have been published (Ali *et al.*, 2016; Asghar *et al.*, 2017, 2018, 2019a; Asghar and Ali, 2019; Asghar *et al.* 2019b; Ali *et al.*, 2019a; Asghar *et al.*, 2019c; Ali *et al.*, 2019b; Javid *et al.*, 2019; Asghar *et al.*, 2020a, b, c).

Unlike aforementioned authors, Pandey and Tripathi (2011a) investigated flow of a micro-polar fluid in a finite tube with the consideration that peristaltic waves do not move beyond the stationary boundary of the tube to match such a flow in oesophagus. Such a wave propagation was designed by Misra and Pandey (2001).

Pandey *et al.* (2017) concluded in their investigation that the wave amplitude does not remain constant during the wave propagation in a peristaltic motion when anything swallows in the oesophagus. The conclusion was derived in order to model the experimental reports of Kahrilas *et al.* (1995) who had located a higher pressure zone in the distal part of the oesophagus in normal as well as pathological state. Pandey and Tiwari (2017) further investigated swallowing

of fluids that match the properties of Casson fluid, due to peristaltic waves of dilating amplitude.

In light of the observation of dilating peristaltic waves by Pandey *et al.* (2017) in oesophagus which validates experimental investigation, peristaltic swallowing of micro-polar fluids (Pandey and Tripathi, 2011a) requires a revisit of investigation. Particularly the impact of dilation of wave amplitude on the non-dimensional parameters such as coupling number and micro-polar parameter may be worth reporting.

## 3.2 Formulation of the problem

We consider the flow of micro-polar fluid in a tube of length of $\tilde{l}$ caused by continuous contraction waves that propagate along the walls of the tube (cf. Figure 3.1), which are given by

$$\tilde{h}(\tilde{x}, \widetilde{\omega}, \tilde{t}) = a - \widetilde{\phi} e^{\widetilde{\omega}\tilde{x}} \cos^2 \frac{\pi}{\lambda}(\tilde{x} - c\tilde{t}), \tag{3.1}$$

where $\tilde{h}, \tilde{x}, \tilde{t}$, $a$, $\widetilde{\phi}, \lambda, \widetilde{\omega}$ and $c$ respectively stand for radial displacement of the wall, axial coordinate, time, radius of the tube, amplitude of the wave, wavelength, dilation parameter and wave velocity (cf. Pandey *et al.* 2017).

The governing equations of the flow of micro-polar fluid in the absence of body forces and body couple are given by

$$\frac{\partial \tilde{u}}{\partial \tilde{x}} + \frac{1}{\tilde{r}}\left(\frac{\partial(\tilde{r}\tilde{v})}{\partial \tilde{r}}\right) = 0 \tag{3.2}$$

$$\rho\left(\frac{\partial\tilde{u}}{\partial\tilde{t}}+\tilde{u}\frac{\partial\tilde{u}}{\partial\tilde{x}}+\tilde{v}\frac{\partial\tilde{u}}{\partial\tilde{r}}\right)=-\frac{\partial\tilde{p}}{\partial\tilde{x}}+k\frac{1}{\tilde{r}}\frac{\partial(\tilde{r}\tilde{w})}{\partial\tilde{r}}+(\mu+k)\left(\frac{\partial^2\tilde{u}}{\partial\tilde{x}^2}+\frac{1}{\tilde{r}}\frac{\partial}{\partial\tilde{r}}\left(\tilde{r}\frac{\partial\tilde{u}}{\partial\tilde{r}}\right)\right), \tag{3.3}$$

$$\rho\left(\frac{\partial\tilde{v}}{\partial\tilde{t}}+\tilde{u}\frac{\partial\tilde{v}}{\partial\tilde{x}}+\tilde{v}\frac{\partial\tilde{v}}{\partial\tilde{r}}\right)=-\frac{\partial\tilde{p}}{\partial\tilde{r}}-k\frac{\partial\tilde{w}}{\partial\tilde{x}}+(\mu+k)\left(\frac{\partial^2\tilde{v}}{\partial\tilde{x}^2}+\frac{\partial}{\partial\tilde{r}}\left(\frac{1}{\tilde{r}}\frac{\partial(\tilde{r}\tilde{v})}{\partial\tilde{r}}\right)\right), \tag{3.4}$$

$$\rho\widetilde{\sigma}\left(\frac{\partial\tilde{w}}{\partial\tilde{t}}+\tilde{u}\frac{\partial\tilde{w}}{\partial\tilde{x}}+\tilde{v}\frac{\partial\tilde{w}}{\partial\tilde{r}}\right)=-2k\tilde{w}+k\left(\frac{\partial\tilde{v}}{\partial\tilde{x}}-\frac{\partial\tilde{u}}{\partial\tilde{r}}\right)+\gamma\left(\frac{\partial^2\tilde{w}}{\partial\tilde{x}^2}+\frac{\partial}{\partial\tilde{r}}\left(\frac{1}{\tilde{r}}\frac{\partial(\tilde{r}\tilde{w})}{\partial\tilde{r}}\right)\right)+(\alpha+\beta+\gamma)\widetilde{\nabla}\left(\widetilde{\nabla}.\tilde{w}\right). \tag{3.5}$$

where $\tilde{u}$, $\tilde{v}$, $\tilde{w}$, $\tilde{r}$, $\rho$, $\widetilde{\sigma}$ are respectively the axial velocity, the radial velocity, the micro-polar vector, the radial coordinate, the fluid density and the micro-gyration parameter. The parameters $\mu$, $k$, $\alpha$, $\beta$, $\gamma$ are material constants satisfying the following conditions:

$$2\mu+k\geq 0,\ \ k\geq 0,\ \ 3\alpha+\beta+\gamma\geq 0,\ \ \gamma\geq\left|\beta\right|. \tag{3.6}$$

The following dimensionless parameters are introduced for the subsequent analysis:

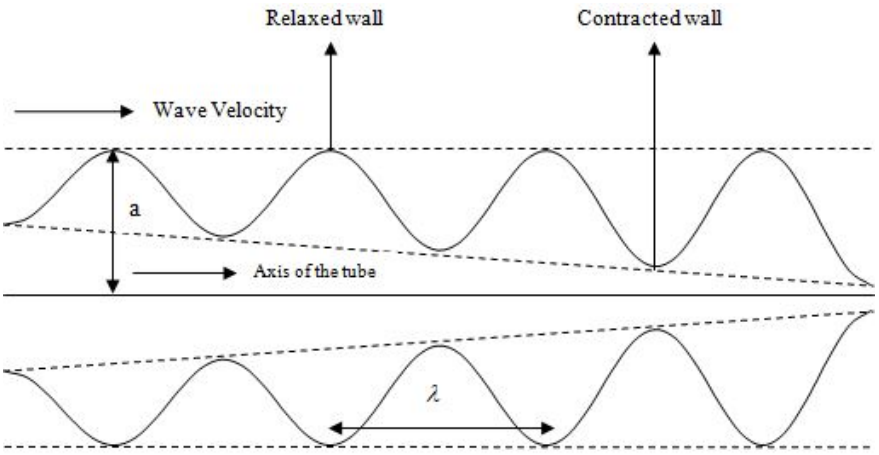


**Figure 3.1:** Schematic diagram of oesophagus, (based on equation (3.16)), represents the propagation of a progressive wave, where $\delta = \frac{a}{\lambda}$, $Re$, $Q$ denote respectively the wave number, the Reynolds number and the volume flow rate.

$$x = \frac{\tilde{x}}{\lambda},\ r = \frac{\tilde{r}}{a},\ t = \frac{c\tilde{t}}{\lambda},\ u = \frac{\tilde{u}}{c},\ v = \frac{\tilde{v}}{c\delta},\ \delta = \frac{a}{\lambda},\ w = \frac{a\tilde{w}}{c},\ h = \frac{\tilde{h}}{a},$$
$$\omega = \widetilde{\omega}\lambda,\ l = \frac{\tilde{l}}{\lambda},\ \phi = \frac{\widetilde{\phi}}{a},\ \sigma = \frac{\widetilde{\sigma}}{a^2},\ p = \frac{\tilde{p}a^2}{\mu c\lambda},\ Re = \frac{\rho ca\delta}{\mu},\ Q = \frac{\tilde{Q}}{\pi a^2 c}. \quad (3.7)$$

Introduction of the dimensionless parameters gets equations (3.2)-(3.5) transformed to

$$\frac{\partial u}{\partial x} + \frac{1}{r}\left(\frac{\partial (rv)}{\partial r}\right) = 0, \quad (3.8)$$

$$Re\delta\left(\frac{\partial u}{\partial t} + u\frac{\partial u}{\partial x} + v\frac{\partial u}{\partial r}\right) = -\frac{\partial p}{\partial x} + \frac{N}{1-N}\frac{1}{r}\frac{\partial (rw)}{\partial r} + \frac{1}{1-N}\left(\delta^2\frac{\partial^2 u}{\partial x^2} + \frac{1}{r}\frac{\partial}{\partial r}\left(r\frac{\partial u}{\partial r}\right)\right), \quad (3.9)$$

$$Re\delta^3\left(\frac{\partial v}{\partial t}+u\frac{\partial v}{\partial x}+v\frac{\partial v}{\partial r}\right)=-\frac{\partial p}{\partial r}+\frac{\delta^2}{1-N}\left(-N\frac{\partial w}{\partial x}+\frac{\partial}{\partial r}\left(\frac{1}{r}\frac{\partial (rv)}{\partial r}\right)+\delta^2\frac{\partial^2 v}{\partial x^2}\right), \quad (3.10)$$

$$\frac{\sigma Re\delta(1-N)}{N}\left(\frac{\partial w}{\partial t}+u\frac{\partial w}{\partial x}+v\frac{\partial w}{\partial r}\right)=-2w+\left(\delta^2\frac{\partial v}{\partial x}-\frac{\partial u}{\partial r}\right)$$
$$+\frac{2-N}{m^2}\left(\frac{\partial}{\partial r}\left(\frac{1}{r}\frac{\partial (rw)}{\partial r}\right)+\delta^2\frac{\partial^2 w}{\partial x^2}\right). \quad (3.11)$$

Employing the long wavelength and low Reynolds number approximations, the dimensionless equations (3.8)- (3.11) reduce to

$$\frac{\partial u}{\partial x}+\frac{1}{r}\left(\frac{\partial (rv)}{\partial r}\right)=0, \quad (3.12)$$

$$\frac{\partial p}{\partial x}=\frac{1}{1-N}\left\{\frac{N}{r}\frac{\partial (rw)}{\partial r}+\frac{1}{r}\frac{\partial}{\partial r}\left(r\frac{\partial u}{\partial r}\right)\right\}, \quad (3.13)$$

$$\frac{\partial p}{\partial r}=0, \quad (3.14)$$

$$2w+\frac{\partial u}{\partial r}-\frac{2-N}{m^2}\frac{\partial}{\partial r}\left(\frac{1}{r}\frac{\partial (rw)}{\partial r}\right)=0. \quad (3.15)$$

where $N=\left(\frac{k}{\mu+k}\right)$ is the coupling number, which is a measure of particle coupling with its surroundings $(0\leq N\leq 1)$, $m=\sqrt{\frac{a^2k(2\mu+k)}{\gamma(\mu+k)}}$ is the micro-polar parameter and $\alpha$, $\beta$ do not appear in the governing equation as the micro-rotation

vector $w$ is solenoidal, i.e. $\nabla \cdot \overrightarrow{w} = 0$. In the limiting case, $k \to 0$ implying $N \to 0$ the governing equations for the micro-polar fluid reduce to the governing equations for Newtonian fluid.

Similarly the wall equation (3.1), under non-dimensionalisation reduce to

$$h(x, \omega, t) = 1 - \phi e^{\omega x} \cos^2 \pi (x - t) \,. \tag{3.16}$$

The following are the boundary conditions imposed on the governing equations:

$$u(x, r, t)|_{r=h} = 0, \quad v(x, r, t)|_{r=h} = \frac{\partial h}{\partial t},$$

$$v(x, r, t)|_{r=0} = 0, \quad \frac{\partial u(x, r, t)}{\partial r}\Big|_{r=0} = 0, \tag{3.17}$$

$$w(x, r, t)|_{r=0} = 0, \quad w(x, r, t)|_{r=H} = 0. \tag{3.18}$$

## 3.3 Solution of the problem

Integration of equation (3.13), once with respect to $r$, yields

$$\frac{\partial u}{\partial r} = (1 - N) \frac{r}{2} \frac{\partial p}{\partial x} - N w + \frac{C_1}{r}, \tag{3.19}$$

Further, integrating equation (3.15) twice with respect to $r$ and also using equation (3.19), we obtain non-homogeneous Bessel equation in the cylindrical coordinates as

$$\frac{\partial^2 w}{\partial r^2}+\frac{1}{r}\frac{\partial w}{\partial r}-\left(m^2+\frac{1}{r^2}\right)w=\frac{m^2}{2-N}\left\{(1-N)\frac{r}{2}\frac{\partial p}{\partial x}+\frac{C_1}{r}\right\}.$$

The general solution of above equation is as follow: (micro-polar vector)

$$w=C_2 I_1(mr)+C_3 K_1(mr)-\frac{1}{2-N}\left\{(1-N)\frac{r}{2}\frac{\partial p}{\partial x}+\frac{C_1}{r}\right\}, \tag{3.20}$$

where $C_1$, $C_2$, $C_3$ are arbitrary functions independent of $r$ and $I_1(mr)$, $K_1(mr)$ are respectively the modified Bessel functions of the $1^{st}$ and the $2^{nd}$ kind of the $1^{st}$ order.

Then applying the fourth boundary condition of equation (3.17), and the boundary conditions (3.18), equations (3.19) and (3.20) become

$$\frac{\partial u}{\partial r}=\frac{1-N}{2-N}\frac{\partial p}{\partial x}\left\{r-\frac{Nh}{2}\frac{I_1(mr)}{I_1(mh)}\right\}, \tag{3.21}$$

$$w=\frac{1-N}{2(2-N)}\frac{\partial p}{\partial x}\left\{\frac{hI_1(mr)}{I_1(mh)}-r\right\}, \tag{3.22}$$

And further integrating equation (3.21) and applying the no-slip condition of equation (3.17), the axial velocity is found as

$$u = \frac{1-N}{2(2-N)}\frac{\partial p}{\partial x}\Big\{r^2 - \phi^2 e^{2\omega x}\cos^4\pi(x-t) + 2\phi e^{\omega x}\cos^2\pi(x-t) - 1 + \frac{Nh}{m}\left(\frac{I_0(mh)-I_0(mr)}{I_1(mh)}\right)\Big\}, \quad (3.23)$$

where $I_0(mr)$, $I_0(mh)$ are the modified Bessel functions of the $1^{st}$ kind and the $0^{th}$ order.

The radial velocity is derived from equation (3.15), by substituting $u$ from equation (3.23) and integrating it once with respect to $r$. The regularity condition, given in equation (3.17), determines the constant term and gives the radial velocity as

$$v = \frac{1-N}{2(2-N)}\Bigg[\frac{\phi e^{\omega x}}{2}\{2\pi\sin 2\pi(x-t) - \omega\cos 2\pi(x-t) - \omega\}\frac{\partial p}{\partial x}\Big\{rh - \frac{N}{m}\Big\{\frac{r}{2}\frac{\partial}{\partial x}\left(\frac{hI_0(mh)}{I_1(mh)}\right) - \frac{I_1(mr)}{m}\frac{\partial}{\partial x}\left(\frac{h}{I_1(mh)}\right)\Big\}\Big\} - \frac{\partial^2 p}{\partial x^2}\Big\{\frac{r^3}{4} - \frac{r}{2}\Big(1 + \phi^2 e^{2\omega x}\cos^4\pi(x-t) - 2\phi e^{\omega x}\cos^2\pi(x-t)\Big) + \frac{Nh}{mI_1(mh)}\left(\frac{r}{2}I_0(mh) - \frac{I_1(mh)}{m}\right)\Big\}\Bigg], \quad (3.24)$$

In order to get pressure gradient, we apply the radial velocity of the wall, given in equation (3.17), on equation (3.24). This gives

$$h\frac{\partial h}{\partial t}=\frac{1-N}{2(2-N)}\Bigg[\frac{\phi e^{\omega x}}{2}\{2\pi\sin 2\pi(x-t)\ -\omega\cos 2\pi(x-t)-\omega\}\frac{\partial p}{\partial x}\Bigg\{1$$
$$-\phi^3 e^{3\omega x}\cos^6\pi(x-t)-3\phi e^{\omega x}\cos^2\pi(x-t)+3\phi^2 e^{2\omega x}\cos^4\pi(x-t)\ -\frac{Nh}{m}$$
$$\left\{\frac{h}{2}\times\frac{\partial}{\partial x}\left(\frac{hI_0(mh)}{I_1(mh)}\right)-\frac{I_1(mh)}{m}\times\frac{\partial}{\partial x}\left(\frac{h}{I_1(mh)}\right)\right\}\Bigg\}+\frac{\partial^2 p}{\partial x^2}$$
$$\left\{\frac{1+\phi^4 e^{4\omega x}\cos^8\pi(x-t)+6\phi^2 e^{2\omega x}\cos^4\pi(x-t)}{4}-\phi e^{\omega x}\cos^2\pi(x-t)\right.$$
$$\left.-e^{3\omega x}\cos^6\pi(x-t)\ +\frac{Nh^2}{2m^2}\left(2-\frac{mhI_0(mh)}{I_1(mh)}\right)\right\}\Bigg], \quad (3.25)$$

Integrating this, with respect to $x$, yields the pressure gradient as

$$\frac{\partial p}{\partial x}=\frac{8(2-N)}{1-N}$$
$$\left\{\frac{\begin{array}{c}G(t)+\frac{\pi\phi}{4}\int_0^x e^{\omega x}\Big[(2\phi e^{\omega x}-4)\sin 2\pi(x-t)\\ +\phi e^{\omega x}\sin 4\pi(x-t)\ \Big]ds\end{array}}{\begin{array}{c}1+\phi^4 e^{4\omega x}\cos^8\pi(x-t)+6\phi^2 e^{2\omega x}\cos^4\pi(x-t)-4\phi e^{\omega x}\cos^2\pi(x-t)\\ -4e^{3\omega x}\cos^6\pi(x-t)\ +\frac{4Nh^2}{m^2}\left(1-\frac{mhI_0(mh)}{2I_1(mh)}\right)\end{array}}\right\}, \quad (3.26)$$

Integrating it once again from 0 to $x$, the pressure is obtained as

$$p(x,\ t)-p(0,\ t)=\frac{8(2-N)}{1-N}$$
$$\int_0^x \frac{G(t)+\frac{\pi\phi}{4}\int_0^s e^{\omega x}\left[(2\phi e^{\omega x}-4)\sin 2\pi(x-t)\ +\phi e^{\omega x}\sin 4\pi(x-t)\ \right]ds_1}{1+\phi^4 e^{4\omega x}\cos^8\pi(x-t)+\ 6\phi^2 e^{2\omega x}\cos^4\pi(x-t)-4\phi e^{\omega x}\cos^2\pi(x-t)} ds,$$
$$-4e^{3\omega x}\cos^6\pi(x-t)\ +\frac{4Nh^2}{m^2}\left(1-\frac{mhI_0(mh)}{2I_1(mh)}\right) \tag{3.27}$$

Substituting $x=l$ in equation (3.27), the pressure between the inlet and the outlet of the tube, is obtained as

$$p(l,\ t)-p(0,\ t)=\frac{8(2-N)}{1-N}$$
$$\int_0^l \frac{G(t)+\frac{\pi\phi}{4}\int_0^x e^{\omega x}\Big[(2\phi e^{\omega x}-4)\sin 2\pi(x-t) +\phi e^{\omega x}\sin 4\pi(x-t)\ \Big]ds}{1+\phi^4 e^{4\omega x}\cos^8\pi(x-t)+\ 6\phi^2 e^{2\omega x}\cos^4\pi(x-t)-4\phi e^{\omega x}\cos^2\pi(x-t)} dx, \tag{3.28}$$
$$-4e^{3\omega x}\cos^6\pi(x-t)\ +\frac{4Nh^2}{m^2}\left(1-\frac{mhI_0(mh)}{2I_1(mh)}\right)$$

where $G(t)$ is a function of $t$ which is evaluated by a simple manipulation as

$$G(t)=\frac{\frac{1-N}{8(2-N)}\Delta p_l(t)-\int_0^l \frac{\frac{\pi\phi}{4}\int_0^x e^{\omega x}[(2\phi e^{\omega x}-4)\sin 2\pi(x-t)\ +\phi e^{\omega x}\sin 4\pi(x-t)\ ]ds}{1+\phi^4 e^{4\omega x}\cos^8\pi(x-t)+\ 6\phi^2 e^{2\omega x}\cos^4\pi(x-t)-4\phi e^{\omega x}\cos^2\pi(x-t)-4e^{3\omega x}\cos^6\pi(x-t)}dx}{\int_0^l \frac{1}{1+\phi^4 e^{4\omega x}\cos^8\pi(x-t)+\ 6\phi^2 e^{2\omega x}\cos^4\pi(x-t)-4\phi e^{\omega x}\cos^2\pi(x-t)-4e^{3\omega x}\cos^6\pi(x-t)}dx}$$
$$+\frac{4Nh^2}{m^2}\left(1-\frac{mhI_0(mh)}{2I_1(mh)}\right)$$
$$+\frac{4Nh^2}{m^2}\left(1-\frac{mhI_0(mh)}{2I_1(mh)}\right), \tag{3.29}$$

where $\Delta p_l(t)=p(l,\ t)-p(0,\ t)$ is the pressure difference between the inlet and outlet of the tube.

The volume flow rate is defined as $Q(x,\ t)=\int_0^h 2rudr$, yields, on performing the integration, the following:

$$Q(x,\ t)=\frac{N-1}{4(2-N)}\frac{\partial p}{\partial x}\Big\{1+\phi^4 e^{4\omega x}\cos^8\pi(x-t)+6\phi^2 e^{2\omega x}\cos^4\pi(x-t)$$
$$-4\phi e^{\omega x}\cos^2\pi(x-t)-4e^{3\omega x}\cos^6\pi(x-t)$$
$$+\frac{4Nh^2}{m^2}\left(1-\frac{mhI_0(mh)}{2I_1(mh)}\right)\Big\}, \tag{3.30}$$

The time-averaged volume flow rate is obtained by averaging the volume flow rate for one time period. This gives

$$\tilde{Q}(x,\ t) = \frac{N-1}{4(2-N)} \int_0^1 \frac{\partial p}{\partial x} \Big\{ 1 + \phi^4 e^{4\omega x} \cos^8 \pi (x-t) + 6\phi^2 e^{2\omega x} \cos^4 \pi (x-t) - 4\phi e^{\omega x} \cos^2 \pi (x-t) - 4e^{3\omega x} \cos^6 \pi (x-t) + \frac{4Nh^2}{m^2} \left( 1 - \frac{mhI_0(mh)}{2I_1(mh)} \right) \Big\} dt, \quad (3.31)$$

The time-averaged volume flow rate may be given in terms of the flow rate in the wave frame, and also in the laboratory frame, as

$$\tilde{Q} = q + 1 - \phi e^{\omega x} + \frac{3}{8}\phi^2 e^{2\omega x},$$

$$= Q - \phi e^{\omega x} - \phi^2 e^{2\omega x} \cos^4 \pi (x-t) + 2\phi e^{\omega x} \cos^2 \pi (x-t) + \frac{3}{8}\phi^2 e^{2\omega x}. \quad (3.32)$$

This helps us express the pressure gradient in terms of the time-averaged volume flow rate. With some manipulations equation (3.30) and (3.32) give

$$\frac{\partial p}{\partial x} = \frac{4(2-N)}{N-1} \left\{ \frac{\tilde{Q} + \phi e^{\omega x} + \phi^2 e^{2\omega x} \cos^4 \pi (x-t) - 2\phi e^{\omega x} \cos^2 \pi (x-t) - \frac{3}{8}\phi^2 e^{2\omega x}}{1 + \phi^4 e^{4\omega x} \cos^8 \pi (x-t) + 6\phi^2 e^{2\omega x} \cos^4 \pi (x-t) - 4\phi e^{\omega x} \cos^2 \pi (x-t) - 4e^{3\omega x} \cos^6 \pi (x-t) + \frac{4Nh^2}{m^2} \left( 1 - \frac{mhI_0(mh)}{2I_1(mh)} \right)} \right\}, \quad (3.33)$$

which yields, on integration, pressure difference in terms of the time-averaged volume flow rate as

$$p(x)-p(0)=\frac{4(2-N)}{N-1}$$
$$\int_0^x \frac{\tilde{Q}+\phi e^{\omega x}+\phi^2 e^{2\omega x}\cos^4\pi(x-t)-2\phi e^{\omega x}\cos^2\pi(x-t) -\frac{3}{8}\phi^2 e^{2\omega x}}{1+\phi^4 e^{4\omega x}\cos^8\pi(x-t)+6\phi^2 e^{2\omega x}\cos^4\pi(x-t)-4\phi e^{\omega x}\cos^2\pi(x-t) -4e^{3\omega x}\cos^6\pi(x-t)+\frac{4Nh^2}{m^2}\left(1-\frac{mhI_0(mh)}{2I_1(mh)}\right)}ds, \quad (3.34)$$

for $x=l$, which gives

$$p(l)-p(0)=\frac{4(2-N)}{N-1}$$
$$\int_0^l \frac{\tilde{Q}+\phi e^{\omega x}+\phi^2 e^{2\omega x}\cos^4\pi(x-t)-2\phi e^{\omega x}\cos^2\pi(x-t) -\frac{3}{8}\phi^2 e^{2\omega x}}{1+\phi^4 e^{4\omega x}\cos^8\pi(x-t)+6\phi^2 e^{2\omega x}\cos^4\pi(x-t)-4\phi e^{\omega x}\cos^2\pi(x-t) -4e^{3\omega x}\cos^6\pi(x-t)+\frac{4Nh^2}{m^2}\left(1-\frac{mhI_0(mh)}{2I_1(mh)}\right)}dx, \quad (3.35)$$

Finally, the local wall shear stress is defined as

$$\tau_w=\frac{\partial u}{\partial r}\Big|_{r=h},$$

Which, by virtue of equation (3.21), takes the form

$$\tau_w = \frac{(1-N)H}{2}\frac{\partial p}{\partial x},$$

and further reduces, in view equation (3.26), to

$$\tau_w = 4(2-N)$$
$$\left\{ \frac{G(t) + \frac{\pi\phi}{4}\int_0^x e^{\omega x}\left[(2\phi e^{\omega x} - 4)\sin 2\pi(x-t) + \phi e^{\omega x}\sin 4\pi(x-t)\right] ds}{1 - \phi^3 e^{3\omega x}\cos^6\pi(x-t) - 3\phi e^{\omega x}\cos^2\pi(x-t) + 3\phi^2 e^{2\omega x}\cos^4\pi(x-t) + \frac{4Nh}{m^2}\left(1 - \frac{mhI_0(mh)}{2I_1(mh)}\right)} \right\}, \quad (3.36)$$

## 3.4 Reflux limit

Reflux is an important phenomenon of peristaltic movement and refers to the presence of fluid particles that move, on the average, in a direction opposite to the net flow in the close vicinity of the wall (Shapiro *et al*. 1969).

For the axi-symmetric case, the dimensional form of the stream function in the wave frame is defined as

$$d\widetilde{\psi} = 2\pi\tilde{R}\left(\tilde{U}d\tilde{R} - \tilde{V}d\tilde{X}\right), \quad (3.37)$$

where $\widetilde{\psi}$, $\tilde{X}, \tilde{R}$, $\tilde{U}$ and $\tilde{V}$ are stream function, the axial and the radial co-ordinates, the velocities components the axial and radial directions respectively.

Using the following transformations between the wave and the laboratory frames, defined as

$$\tilde{X} = \tilde{x} - c\tilde{t},\ \tilde{R} = \tilde{r},\ \tilde{U} = \tilde{u} - c,\ \tilde{V} = \tilde{v},\ \tilde{q} = \tilde{Q} - c\tilde{h}^2,\ \widetilde{\Psi} = \widetilde{\psi} - \tilde{r}^2, \tag{3.38}$$

where the left side of the parameters is in the wave frame while the right side of the parameters are in the laboratory frame, we obtain stream function as

$$\psi = -r^2 - \left[ \frac{\begin{array}{c}\left(\tilde{Q} + \phi e^{\omega x} + \phi^2 e^{2\omega x}\cos^4\pi(x-t) - 2\phi e^{\omega x}\cos^2\pi(x-t)\right. \\ \left. -\frac{3}{8}\phi^2 e^{2\omega x}\right)\left\{r^4 - 2r^2H^2 + \frac{2Nh\left(mI_0(mh)r^2 - 2rI_1(mr)\right)}{m^2 I_1(mh)}\right\}\end{array}}{\begin{array}{c}1 + \phi^4 e^{4\omega x}\cos^8\pi(x-t) + 6\phi^2 e^{2\omega x}\cos^4\pi(x-t) - 4\phi e^{\omega x}\cos^2\pi(x-t) \\ -4e^{3\omega x}\cos^6\pi(x-t) \\ +\frac{4Nh^2}{m^2} \times \left(1 - \frac{mhI_0(mh)}{2I_1(mh)}\right)\end{array}} \right], \tag{3.39}$$

Stream function at the wall, $\psi_w$ is solved from equation (3.39) by substituting $r = H$. A simplification yields

$$\psi|_{r=H} = \psi_w = \tilde{Q} - 1 + \phi e^{\omega x} - \frac{3}{8}\phi^2 e^{2\omega x}, \tag{3.40}$$

Reflux flow rate, $Q_\psi(x)$ associated with a particle at the position $x$ is given by

$$Q_\psi(x) = \psi + r^2(\psi,\ x), \tag{3.41}$$

which, on averaging over one cycle, gives

$$\tilde{Q}_\psi = \psi + \int_0^1 r^2(\psi,\ x)dx, \tag{3.42}$$

Moreover, in order to evaluate the reflux limit, $\tilde{Q}_\psi$ is expanded in a power series, in terms of a small parameter $\varepsilon$ about the wall, where $\varepsilon\left(=\psi-\psi_w\right)$ is subjected to the reflux condition

$$\frac{\tilde{Q}_\psi}{\tilde{Q}} > 1 \quad \text{as} \qquad \varepsilon \to 0, \tag{3.43}$$

The coefficient of the first two terms in the expansion of $r$ is obtained only for small values of $m$. Substituting the expansion $r^2(\psi,x) = h^2 + a_1\varepsilon + a_2\varepsilon^2 + a_3\varepsilon^3 + \ldots$ into equation (3.39), and using equation (3.40), we get

$$a_1 = -1, \tag{3.44}$$

$$a_2 = -\left[\frac{\begin{array}{c}\left(1-\frac{1}{4}\frac{mNh}{I_1(mh)}\right)\left(\tilde{Q}+\phi^2 e^{2\omega x}\cos^4\pi(x-t)-2\phi e^{\omega x}\cos^2\pi(x-t)\right.\\ \left.+\phi e^{\omega x}-\frac{3}{8}\phi^2 e^{2\omega x}\right)\end{array}}{\begin{array}{c}1+\phi^4 e^{4\omega x}\cos^8\pi(x-t)+6\phi^2 e^{2\omega x}\cos^4\pi(x-t)-4\phi e^{\omega x}\cos^2\pi(x-t)\\ -4e^{3\omega x}\cos^6\pi(x-t)\\ +\frac{4Nh^2}{m^2}\left(1-\frac{mhI_0(mh)}{2I_1(mh)}\right)\end{array}}\right], \quad (3.45)$$

Then integrating equation (3.41) with respect to $x$ and using equations (3.42)-(3.45), we obtain the reflux limit (i. e. The occurrence of the reflux) as

$$\tilde{Q} < 1-\phi e^{\omega x}+\frac{3}{8}\phi^2 e^{2\omega x} - \frac{\int_0^1 \frac{\left(1-\frac{1}{4}\frac{mNh}{I_1(mh)}\right)}{1+\phi^2 e^{2\omega x}\cos^4\pi(x-t)-2\phi e^{\omega x}\cos^2\pi(x-t)+\frac{4N}{m^2}\left(1-\frac{mhI_0(mh)}{2I_1(mh)}\right)}dx}{\int_0^1 \frac{\left(1-\frac{1}{4}\frac{mNh}{I_1(mH)}\right)}{\begin{array}{c}1+\phi^4 e^{4\omega x}\cos^8\pi(x-t)+6\phi^2 e^{2\omega x}\cos^4\pi(x-t)-4\phi e^{\omega x}\cos^2\pi(x-t)\\ -4e^{3\omega x}\cos^6\pi(x-t)+\frac{4Nh^2}{m^2}\left(1-\frac{mhI_0(mh)}{2I_1(mh)}\right)\end{array}}dx}, \quad (3.46)$$

where $h$ has been given by equation (3.16).

## 3.5 Results and Discussion

In order to explore the effects of various parameters such as coupling number, micro-polar parameter, wave amplitude dilation parameter and the wall shear stress on swallowing of micro-polar fluid, we plot graphs for local pressure distribution along the axis. In order to examine the contribution exclusively of peristalsis, pressure of zero magnitude is prescribed at the two ends of oesophagus, which makes $\Delta p_l(t) = 0$. At a particular time, only one bolus moves in the oesophagus, which is easily experienced when a non-Newtonian fluid swallows. Therefore, for analysis, we consider a single bolus swallowing in the tube which has the capacity to accommodate three boluses at a time; so far our discussion is concerned.

The fundamental motive is to study the local pressure distribution along the axis when a bolus travels down the oesophagus towards the cardiac sphincter. Since the mathematical model involves expressions that cannot be integrated by classical methods, the only way out is to go for numerical evaluation. Moreover, the values of all the non-dimensional parameters are merely suitable assumptions to facilitate qualitative investigation.

### 3.5.1 Effect of dilating wave amplitude on pressure

The bolus is supposed to be already there in the tube at $t = 0.00$. Dashed line symmetric about the axis of the tube are drawn to indicate the position of the bolus in the direction left to right. Fall of pressure from the left towards right paves way for the bolus to move in the tube. Different inclinations of the pressure curve indicate different pressure gradients of the corresponding part of the bolus.

Its gradual rise from the head of the bolus to the end of the tube is the revelation that the motion is under control; the bolus is never let move freely.

The effect of dilating wave amplitude $\omega$ on the flow dynamics is plotted in Figure 3.2. we fix the various parameters $l = 3$, $\phi = 0.7$, $N = 0.10$, $m = 1.0$, and let $\omega$ vary. Fall and rise of pressure throughout the length of the tube from $t = 0.00$ to $t = 2.00$ in the plots is observed to be dependent on the wave amplitude $\omega$, $\omega = 0.00$ corresponding to the constant amplitude ( Figure 3.2). Variation between the maximum and the minimum pressures becomes larger when wave-amplitude dilates, e.g., when $\omega = 0.01,\ 0.02$ (Figure 3.2 ). An observation of Figures ((3.2a) - (3.2f)) reveals that pressure gradients, corresponding to $\omega = 0.01$ and $\omega = 0.02$, are greater in magnitude in the lower oesophageal part than that in the upper oesophageal part and also, if we measure the magnitude, the pressure rises more in the lower part of the oesophagus. It confirms the experimental observations of high pressure zone in the lower oesophageal part even when the fluid transport is of micro-polar nature (Kahrilas *et al*. 1995).

### 3.5.2 Effect of Coupling Number on pressure

Plots in Figure 3.3 depict the impact of the coupling effect parameter $N$, a measure of particle coupling with its surroundings, on pressure distribution along the axis of the tube. We set the various parameters as $l = 3$, $\phi = 0.7$, $\omega = 0.01$, $m = 1.0$ and let $N$ vary in the range $0 - 0.75$.

It is observed that pressure gradient as well as pressure along the length of the oesophagus increases as the coupling effect parameter $N$ increases throughout the length of the tube.

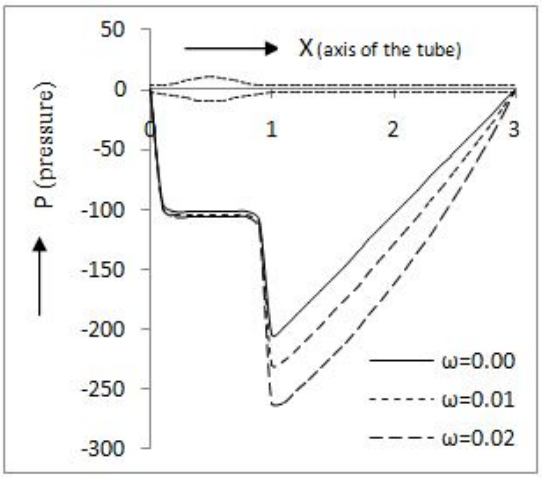


(3.2a) $t = 0.00$

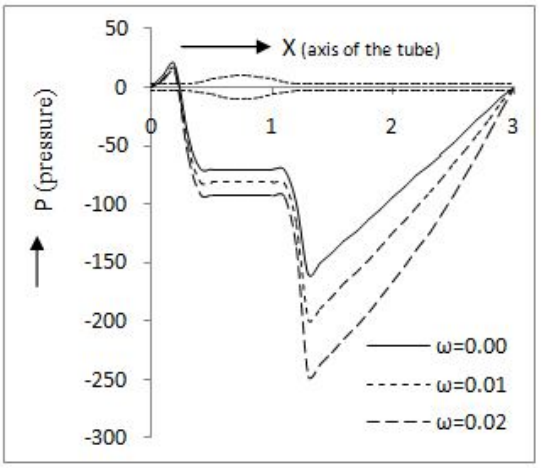


(3.2b) $t = 0.25$

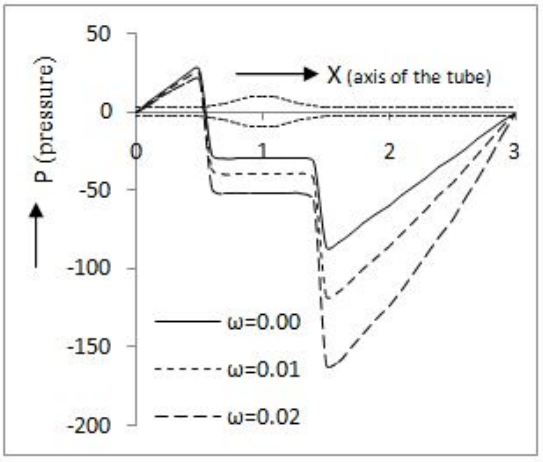


(3.2c) $t = 0.50$

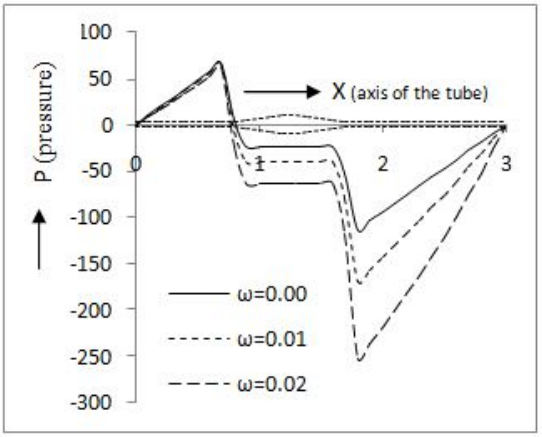


(3.2d) $t = 0.75$

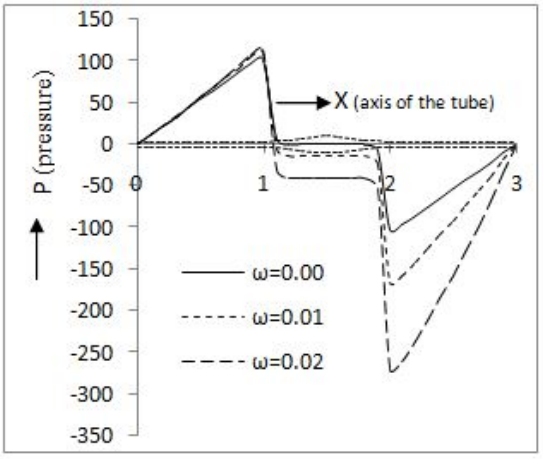


(3.2e) $t = 1.00$

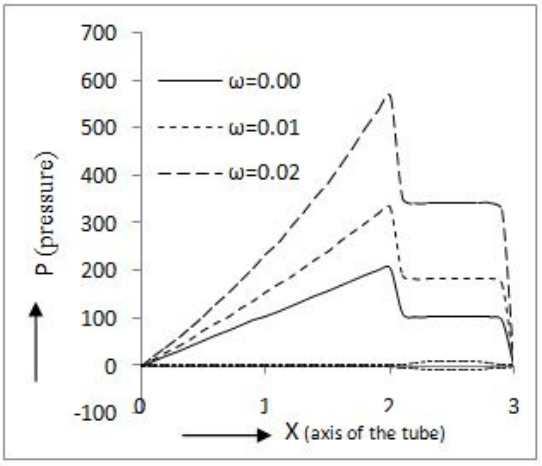


(3.2f) $t = 2.00$

**Figure 3.2:** Pressure distribution along axial distance at different time instants showing the effect of dilation parameter $\omega$. Other parameters are taken as $l = 3$, $\phi = 0.7$, $N = 0.10$, $m = 1.0$.

This may be physically interpreted as that internal rotation of the fluid particles increases pressure; and finally the fluid reduces to Newtonian, i.e. as $N \to 0$, pressure is minimum. This lead to the conclusion that phyically the oesophagus has to make additional efforts to swallow a micro-polar fluid. Similar is the observation for all values of $t$ ranging from $0 \to 2$, i.e., throughout swallowing. Temporal effects are similar to those observed for other fluids such as Newtonian, power-law, visco-elastic, visco-plastic and magneto hydrodynamic fluids (Misra and Pandey, 2001; Pandey and Tripathi, 2010). Figures, together with captions, provide the details (cf. Figure 3.3 ). Achalasia causes inadequate lower oesophageal sphincter relaxation; as a consequence of which oesophageal clearance is delayed. A possible treatment for patients with inadequate lower oesophageal sphincter relaxation is through drugs or by operation (Spechler and Castell, 2001). Thus, this problem will be more acute if the fluid is micro-polar.

### 3.5.3 Effect of micro-polar parameter on pressure

Our next analyse the role of the other micro-polar parameter $m$ by setting other parameters $l = 3$, $\phi = 0.7$, $\omega = 0.01$, $N = 0.50$ and vary $m$ in the rane $1.0 - 5.0$. It is noticed that the pressure along the entire length of the tube decreases as $m$ increases. Hence, this parameter has an opposite effect vis-à-vis coupling number $N$ (cf. Figure 3.3). Since no value of $m$ can lead to Newtonian nature, no comparison can be made with Newtonian fluids. In fact, the micro-polar fluid has a complicated characteristic that is built up by the combined effects of several parameters. This may be recorded that once $N$ vanishes; $m$ no longer exits (cf. Figure 3.4).

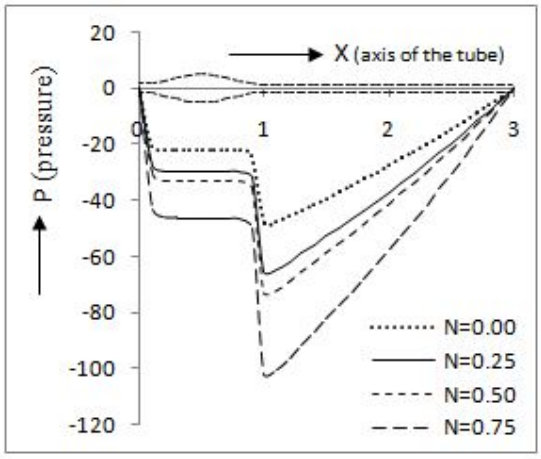


(3.3a) $t = 0.00$

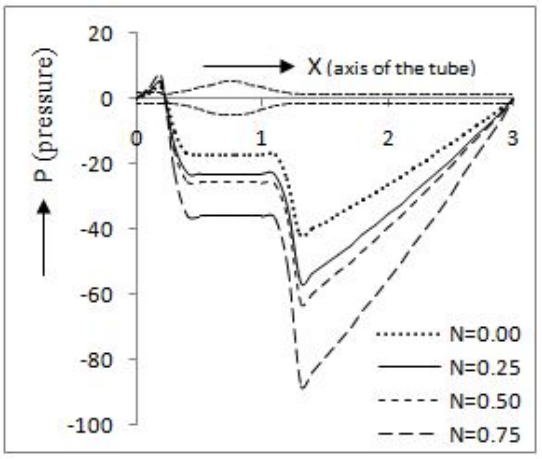


(3.3b) $t = 0.25$

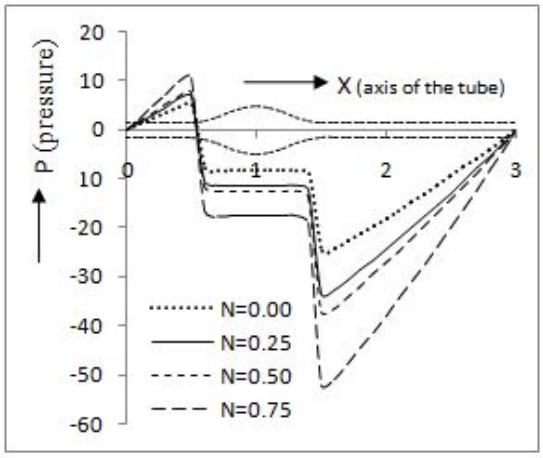


(3.3c) $t = 0.50$

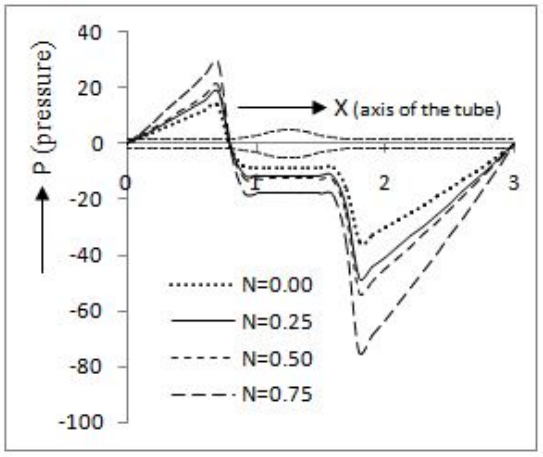


(3.3d) $t = 0.75$

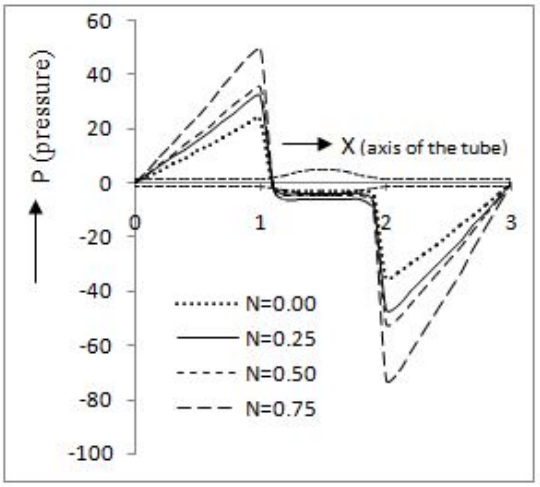


(3.3e) $t = 1.00$

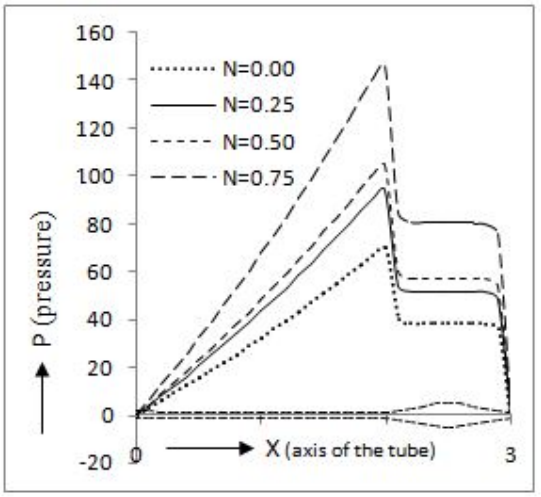


(3.3f) $t = 2.00$

**Figure 3.3:** Pressure distribution along axial distance at different time instants showing the effect of coupling number $N$. Other parameters are set as $l = 3$, $\phi = 0.7$, $\omega = 0.01$, $m = 1.0$

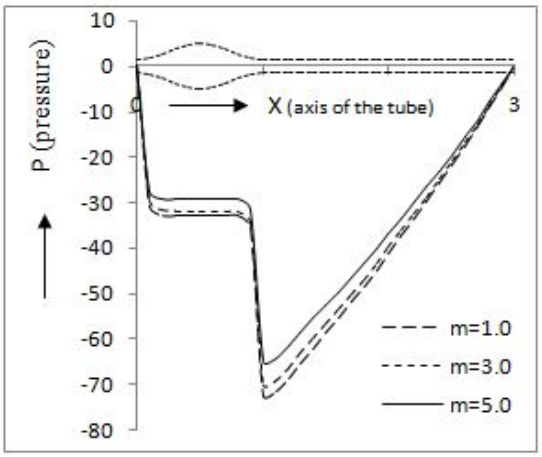


(3.4a) $t = 0.00$

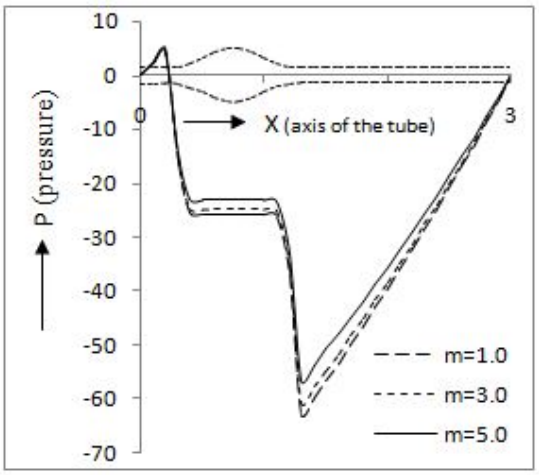


(3.4b) $t = 0.25$

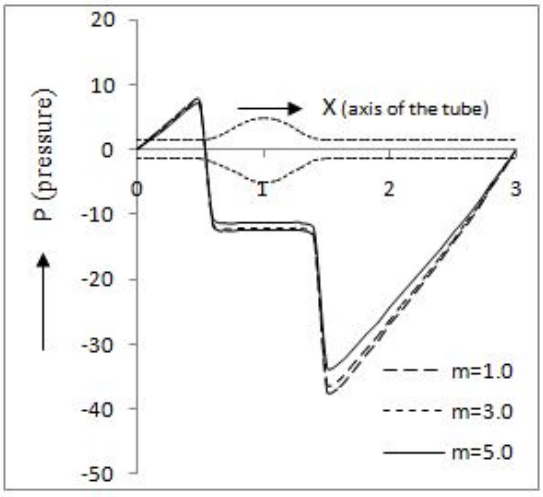


(3.4c) $t = 0.50$

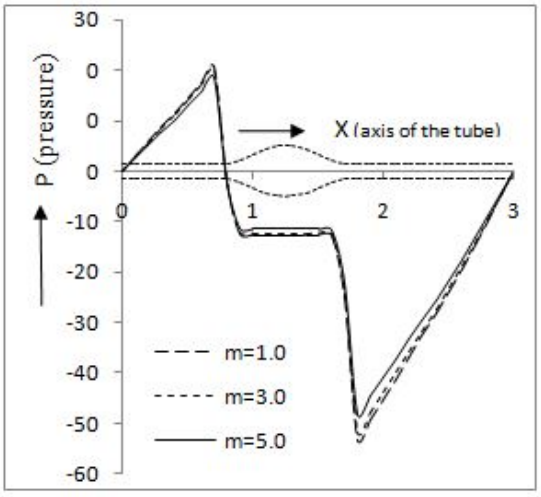


(3.4d) $t = 0.75$

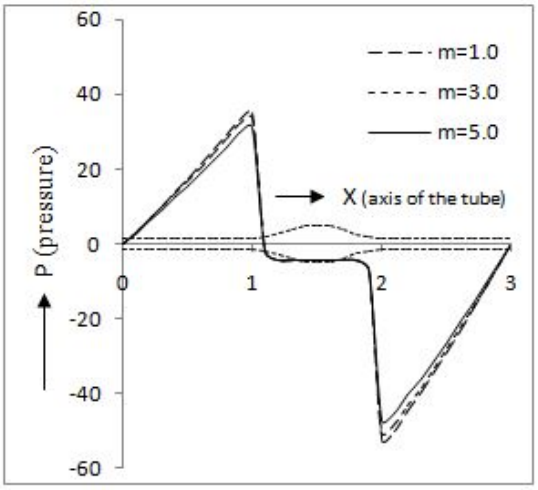


(3.4e) $t = 1.00$

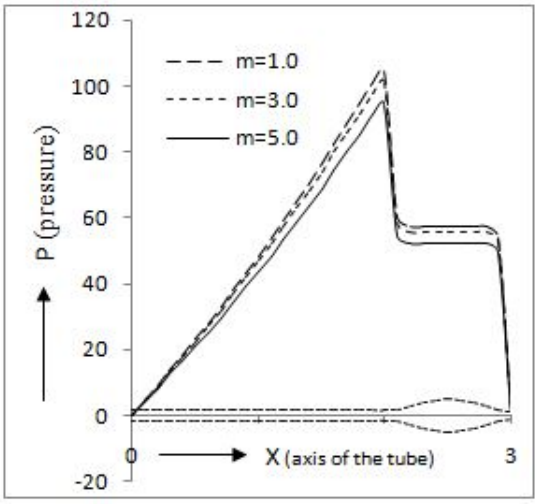


(3.4f) $t = 2.00$

**Figure 3.4:** Pressure distribution along axial distance at different time instants showing the effect of micro polar parameter $m$. Other parameters are taken as $l = 3$, $\phi = 0.7$, $\omega = 0.01$, $N = 0.50$.

### 3.5.4 Effect of dilating wave amplitude on wall shear stress

Figures 3.5 depict the temporal effects of dilating wave amplitude $\omega$ on wall shear stress $\tau_w$ along the length of the tube for distinct values of $t = 0.00 \rightarrow 2.0$. It is observed that the local wall shear stress $\tau_w$ increases with the dilating wave amplitude $\omega$. We found that the bolus felt too much stress, more than double, at $t = 2.0$ instead of $t = 0.00$. Therefore, in the lower part of the oesophagus, bolus will experience higher pressure to transport the bolus in the human oesophagus. Due to the high stress, the size of bolus looks shrunk in the lower part of the human oesophagus (Kahrilas *et al.*, 1995).

## 3.6 Effect of dilating wave amplitude on reflux

Flow rate enhances when wave amplitude is increased. Shapiro *et al.* (1969) discovered retrograde motion corresponding to a given wave amplitude. Less flow rate across a cross section than that across a smaller area within the same cross section is an indication of retrograde motion. In such a case, some fluid flows in the opposite direction near the tubular wall. Consequently, the amount of flow diminishes. This is because close to the inner the periphery, flow is in the reverse direction diminishing the net flow as expected. The flow rate, beyond which there is no reflux, was termed as reflux limit. For small and large amplitudes, Shapiro *et al.* (1969) used different perturbation techniques to estimate the limits.

The analysis for large amplitude and high flow rates has been carried out. Pandey and Tripathi (2011b) observed that micro-polar fluids are more prone to reflux. The curves representing reflux limits for micro-polar fluids are

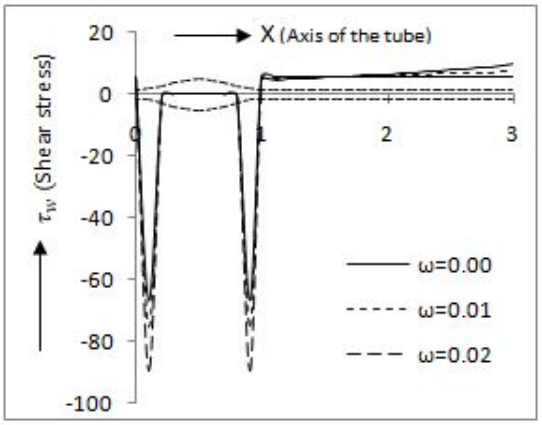


(3.5a) $t = 0.00$

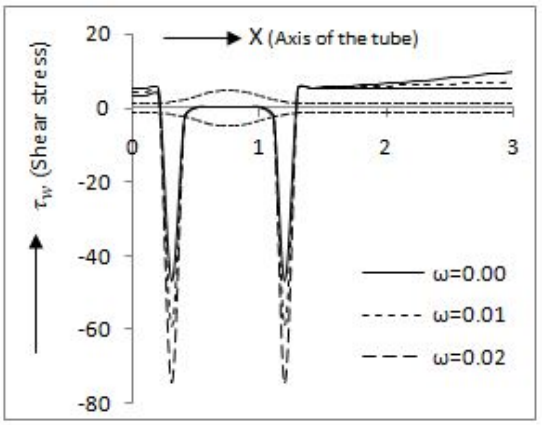


(3.5b) $t = 0.25$

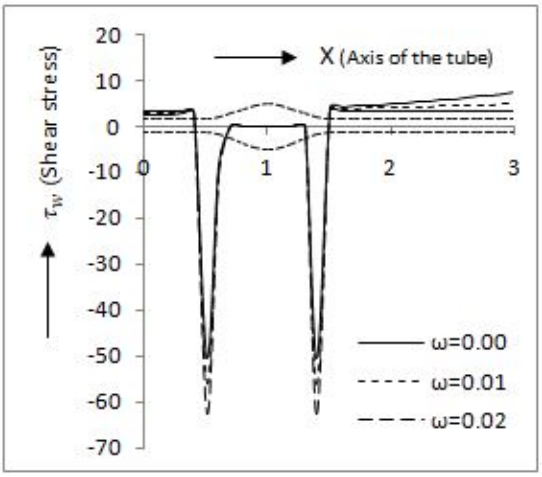


(3.5c) $t = 0.50$

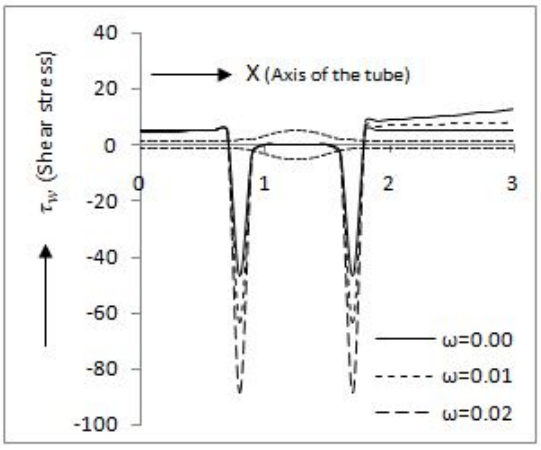


(3.5d) $t = 0.75$

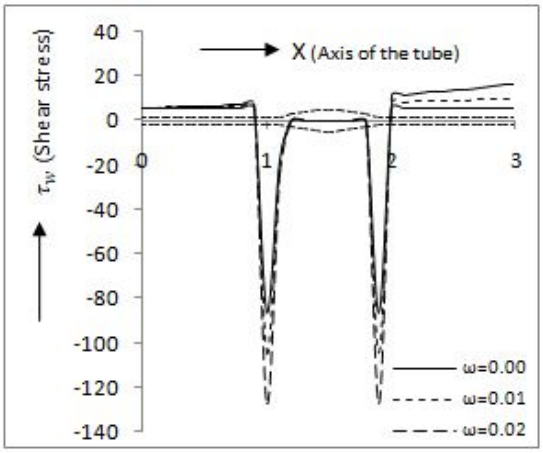


(3.5e) $t = 1.00$

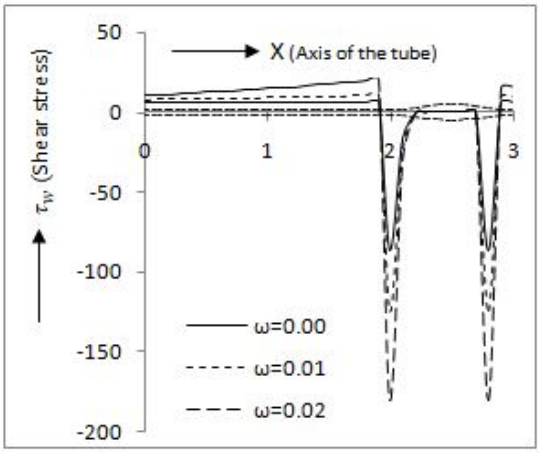


(3.5f) $t = 2.00$

**Figure 3.5:** Wall shear stress $\tau_w$ distribution along axial distance at different time instants showing the effect of dilation parameter $\omega$. Other parameters are taken as $l = 3$, $\phi = 0.7$, $N = 0.10$, $m = 1.0$.

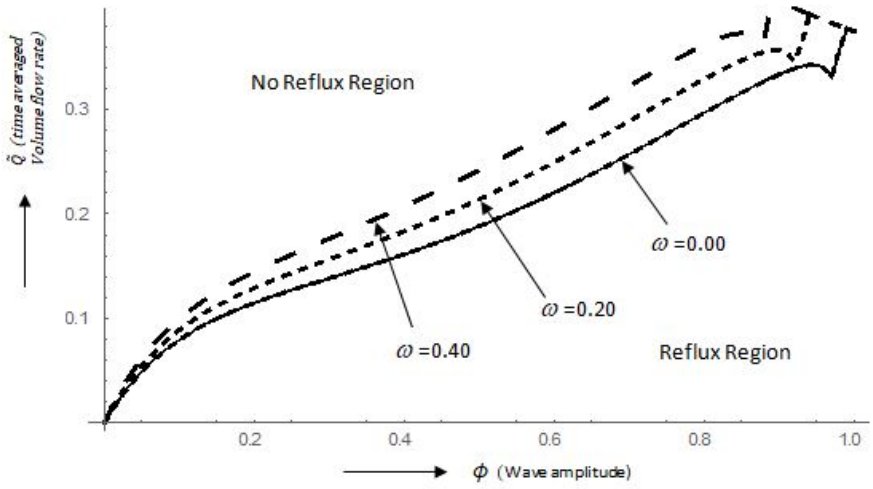


**Figure 3.6:** The diagram exhibits the relation between time averaged flow rate $\tilde{Q}$ and wave amplitude $\phi$ showing the effect of dilation parameter $\omega$. Other parameters are taken as $N = 0.10,\ m = 1.0$.

higher compared to that of Newtonian fluid, for low flow rates. In order to examine the role of dilating amplitude, we fix the coupling number and micro-polar parameter as $N = 0.10$, $m = 1.0$, and then vary the dilating parameter by plotting the time averaged flow rate against wave amplitude. The curves indicate that as the amplitude increases more flow rates required for reflux to take place. We further observed that the curve corresponding to reflux limit rises as wave amplitude is augmented with the dilating parameter of higher magnitude (Figure 3.6), clearly indicating that reflex actions weakens with dilating wave amplitude. Only higher flow rates may cause reflux. Thus, dilating amplitude saves flow from retrograde motion in the oesophagus.

## 3.7 Conclusion and Physical Interpretation

The objective of this analysis is to learn the effect of dilating wave amplitude on the non-Newtonian nature of fluid, which is swallowed in the oesophagus.

Here, the non-Newtonian nature is characterized by the micro-polar parameter and coupling number. These characteristics give it the name micro-polar fluid. It is found that the presence of coupling number and micro-polar parameter requires more pressure to be exerted by the wall of the oesophagus on the fluid swallowing inside it. Dilating wave amplitude increases it further. This confirms the experimental observations (Kahrilas *et al*. 1995) of high pressure zone in the lower part of the oesophagus.

The micro-polar and Newtonian fluids have qualitatively similar pressure distributions; but differences in magnitudes are very much significant. The acknowledgment is that coupling number $N$ and dilation parameter $\omega$ increase pressure along the entire length of the oesophagus, while the other micro-polar parameter $m$ decreases it.

It is observed that for exponentially increasing wave-amplitude, pressure increases along the entire length of the oesophagus; and finally towards the end of the oesophageal flow, it is at the peak. It is found that the pressure distribution is dependent on the position of the wave that propagates in the oesophagus. The local rate of change in the pressure difference is much greater when the wave originates at the inlet and terminates at the outlet of the oesophagus than when the wave lies midway. This may be associated to the fact that the pumping action does not take place along the entire length of the oesophagus uniformly. The rate of change is higher in the proximity of the inlet and the outlet. This present investigation prohibits feeding of micro-polar fluids to the patients suffering from achalasia.

It is also concluded that for the non-Newtonian micro-polar fluids, reflux is less probable with increasing amplitude and further augmented by the dilation parameter.

**********